Brittleness, ductility, and the Griffith crack

Ritva Löfstedt
Institute for Theoretical Physics, University of California, Santa Barbara, California 93106
(Received 10 October 1996)

The material properties which determine whether a solid will fail by brittle fracture or ductile deformation are theoretically investigated by including the leading-order dissipative term describing plastic flow in the equations of elasticity. In particular, this term yields a time scale for the blunting of the elastic crack tip described by Griffith. This time scale is compared to the elastic response time of a solid to determine whether the solid will sustain the high stresses characteristic of a crack tip or will plastically relax the elastic strains. These dissipative equations of elasticity also describe the ''work-hardened'' state of a solid, where brittle fracture becomes possible in an originally ductile solid. [S1063-651X(97)10406-8]

PACS number(s): 05.70.Ln, 62.20.Hg, 62.20.Fe, 81.40.Lm

Despite their obvious engineering relevance, the concepts of brittleness and ductility remain only empirically and phenomenologically defined. Brittle materials fail by crack-induced fracture while in ductile ones voids grow, coalesce, and multiply to weaken the solid. In an effort to quantify this difference, this paper discusses the stability of a crack tip against plastic deformation. By including the leading-order dissipative term characteristic of elastic solids, the time scale appropriate to plastic relaxation of the elastic strains at a crack tip is compared to the speed of the elastic response itself. This comparison determines whether the large stresses characteristic of brittle fracture can be sustained in the solid or whether the solid yields plastically to the externally imposed forces. In addition the dissipative term in elasticity admits a solution which describes a ''work-hardened'' state, where brittle fracture can occur even in an originally ductile solid.

The modern theory of fracture mechanics is based on the calculation by Inglis [1] of the stresses and strains surrounding an elliptical hole in an elastic plane stressed at infinity. His solution indicates the geometrical enhancement of the externally imposed stress at the tips of the elliptical shape. Griffith [2] used this solution to analyze the strength of materials, which most frequently fracture at imposed stresses orders of magnitude below the theoretically predicted values. Griffith postulated that microscopic flaws, in the form of cracks, focus the applied tension to exceed the elastic strength of the solid and cause the failure of the material. By comparing the observed and calculated tensile strengths of glass, Griffith reconciled these observations by calculating the typical size of intrinsic flaws.

The Inglis solution, as presented in elliptical coordinates defined by $x+iy=c\ \cosh(\alpha+i\beta)$, where c is the focal length of the ellipse, is as follows:

$$\sigma_{\alpha\alpha}=T\,\frac{\sinh 2\alpha(\cosh 2\alpha-\cosh 2\alpha_0)}{(\cosh 2\alpha-\cos 2\beta)^2}, \tag{1}$$

$$\sigma_{\beta\beta}=T\,\frac{\sinh 2\alpha(\cosh 2\alpha+\cosh 2\alpha_0-2\cos 2\beta)}{(\cosh 2\alpha-\cos 2\beta)^2}, \tag{2}$$

$$\sigma_{\alpha\beta}=T\,\frac{\sin 2\beta(\cosh 2\alpha-\cosh 2\alpha_0)}{(\cosh 2\alpha-\cos 2\beta)^2}, \tag{3}$$

where σ_{ij} is the force in the j direction per unit surface perpendicular to the i direction, T is the (isotropic) tension imposed at infinity, and α_0 denotes the surface of the elliptical void. These solutions satisfy the boundary conditions of vanishing shear stress and perpendicular stress at the surface, and correspond to displacements given by

$$\delta R_a=\frac{1}{h}\,\frac{c^2T}{8\mu}\,[(p-1)\cosh 2\alpha-(p+1)\cos 2\beta+2\cosh 2\alpha_0] \tag{4}$$

and $\delta R_\beta=0$. Here h is the modulus of the transformation to elliptical coordinates, viz., $h=c\sqrt{(\cosh 2\alpha-\cos 2\beta)/2}$, μ is the shear modulus of the material, and $p=3-4\sigma$ for plane strain, where σ is Poisson's ratio. This solution is depicted in Fig. 1.

The stress concentration is apparent by evaluating $\sigma_{\beta\beta}$, Eq. (2), at the tip of the ellipse ($\alpha=\alpha_0$, $\beta=0$), which finds $\sigma_{\beta\beta}=2Ta/b$, where a and b are the major and minor axes of the ellipse, respectively. As the ellipse becomes more slender, the stress concentration at the tip grows larger. The stress in the perpendicular direction ($\sigma_{\alpha\alpha}$) is forced to vanish right at the surface, but one can readily use the solution (1) above to calculate where this stress reaches its maximum. For slender ellipses, the maximum stress along the major axis is reached at $\alpha=\alpha_0+(1+\sqrt{3})b/a$, and there $\sigma_{\alpha\alpha}\approx T(2a/9b)$. As the ellipse becomes more cracklike, the

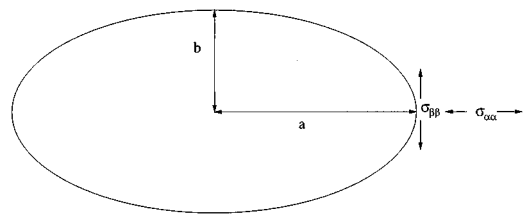

FIG. 1. The Inglis solution for an elliptical void in a uniformly stressed plane. The stress at infinity is amplified at the crack tip, where the tensile stress reaches a maximum $2T(a/b)$. The perpendicular stress is forced to vanish at the surface, but for sufficiently narrow ellipses reaches a maximum value of $T(2a/9b)$ just ahead of the crack tip.

point of maximum stress in the perpendicular direction moves closer to the surface, but the maximum stress in the perpendicular direction remains smaller than the maximum tensile stress. In Griffith's model of fracture, the crack assumes an aspect ratio (a/b) such that the tensile stress at the crack tip precisely equals the cohesive strength of the solid, i.e., $a/b \approx \mu_c/T$, where μ_c is the cohesive strength of the solid. If the cohesive strength scales as the bulk modulus, an assumption supported by both measurements and simple phenomenological arguments for the strength of a solid, this relation simplifies to $a/b \approx \mu/T$. This latter criterion for the aspect ratio is also the one set by requiring that in the absence of external forces the solid should close up and become whole. This translates into setting the displacement of the solid at the end of the minor axis ($\alpha = \alpha_0$, $\beta = \pi/2$) equal to its current location b. Since Griffith's experimental observations found an experimental yield stress in glass roughly 400 times smaller than the theoretically predicted one, he assumed that internal cracks focused the external stresses by this amount. He then reasoned that intrinsic defects in the glass under investigation should have an aspect ratio of that order. By assuming that the smallest radius of curvature $\rho_c = (b^2/a)$ possible in a solid corresponds to an atomic size, i.e., measured in Angströms, Griffith found that the intrinsic cracks in his glass specimens were 1 μm long.

Griffith's model of fracture rests on the assumption that the tendency for elastic solids is to focus large stresses and strains at the crack tip. However, beyond certain stress levels solids typically display plastic deformation [3] and resist increasing strain, and even at low stress levels creep and relaxation mechanisms act to slowly diminish elastic stresses [4]. To describe how elastic strains may be plastically relaxed and to address the question of the stability of a crack tip against plastic deformation I will include the leading-order dissipative term in the equations of elasticity. This term, which describes the diffusion of dislocations through a solid, depends both on the elastic stresses and on specific material properties, which may be rate and history dependent. Once these material-specific properties are identified, one can measure them in macroscopic experimental systems where plastic effects form merely a perturbative correction to the elastic fields. Such systems include creep experiments which measure the slow plastic deformation due to small longitudinal, torsional, and bending loads. Given the elastic solution which describes a crack Eqs. [(1)–(4)] and the (experimentally measured) dissipative equations of state one can determine whether elastic or plastic effects dominate at the crack tip. Specifically one might predict the circumstances under which an elliptical shape will sharpen towards the cracklike limit or blunt so as to prevent brittle fracture.

Equations (1)–(4) above are solutions to the classical equations of elasticity [5]:

$$\frac{\partial \rho}{\partial t} + \vec{\nabla} \cdot \rho \vec{\nu} = 0, \tag{5}$$

which expresses conservation of mass,

$$\frac{\partial \rho \nu_i}{\partial t} + \frac{\partial}{\partial r_j} (\rho \nu_i \nu_j + P \delta_{ij} + \tau_{ij}) = 0, \tag{6}$$

which expresses conservation of momentum,

$$\frac{\partial \rho s}{\partial t} + \vec{\nabla} \cdot \rho s \vec{\nu} = 0, \tag{7}$$

which expresses conservation of entropy, and

$$\frac{\partial R_i}{\partial t} + (\vec{\nu} \cdot \vec{\nabla}) R_i = 0, \tag{8}$$

which describes how the lattice distorts. In these equations, $\rho(\vec{r},t)$ is the density, $\vec{\nu}(\vec{r},t)$ is the velocity, $s(\vec{r},t)$ is the entropy per gram, and $\vec{R}(\vec{r},t)$ is the position at time 0 of a lattice point which at time t is at $\vec{r}$. By requiring energy conservation, one can derive expressions for the pressure,

$$P = \kappa \vec{\nabla} \cdot (\vec{R} - \vec{r}),$$

and the shear stress tensor,

$$\tau_{ij} = \mu \left(\frac{\partial R_i}{\partial r_j} + \frac{\partial R_j}{\partial r_i} - \frac{2}{3} (\vec{\nabla} \cdot \vec{R}) \delta_{ij} \right),$$

where κ and μ are the bulk and shear moduli, respectively. In Eqs. (1)–(4), $\sigma_{ij} = P \delta_{ij} + \tau_{ij}$ and $\delta \vec{R} = \vec{r} - \vec{R}$. The equations of elasticity, Eqs. (5)–(8), differ from the Euler equations of fluid mechanics by the existence of the shear stress tensor, and the subsequent need for Eq. (8) to close the equations.

Eckart [6] introduced a general method of calculating the lowest-order dissipative fluxes corresponding to a macroscopic continuum theory by requiring that energy be conserved and that entropy production be positive. For an Eulerian fluid, this method yields the familiar terms describing viscosity and thermal conductivity, and thus ''derives'' the Navier-Stokes equations. Applied to the equations of elasticity, this method yields in addition to viscosity and thermal conductivity, which shall henceforth be neglected, a damping term unique to solids [6–8] which modifies Eq. (7) as

$$\frac{\partial \rho s}{\partial t} + \vec{\nabla} \cdot \rho s \vec{\nu} = d \left(\frac{\partial \tau_{ij}}{\partial r_j} \right)^2, \tag{9}$$

and Eq. (8) as

$$\frac{\partial R_i}{\partial t} + (\vec{\nu} \cdot \vec{\nabla}) R_i = d \frac{\partial \tau_{ij}}{\partial r_j}. \tag{10}$$

Here d is a diffusion constant, which we assume is proportional to the number of dislocations in the solid, so that a perfect lattice will not plastically distort. This additional term describes the diffusion of dislocations through the lattice, which flow in response to gradients in the shear stress. [Note that in Eqs. (9) and (10) viscoelastic terms, which imply an exponential relaxation of elastic shear stresses on some characteristic time scale, have been suppressed. The viscoelastic dissipative terms, which follow from thermodynamic arguments similar to those above [6,8], render the elastic solid unable to maintain any shear stress. In that sense, Eqs. (9) and (10) represent the leading-order dissipative contribution to the robust elastic solid state, which supports a uniform shear; that is the regime of interest for this analysis.]

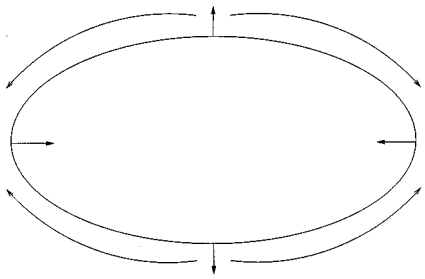

FIG. 2. The plastic flow associated with the Inglis crack. The tendency of the plastic flow is to deform the elliptical void into a circle, which acts to blunt the crack tip. The rate of blunting at the crack tip is approximately given by $a/\dot{a} \approx b^2/\mu d$. If this time scale is shorter than the elastic response time, the solid will not support a crack and will deform in a ductile, rather than brittle, fashion.

Since Eq. (10) contains a higher derivative than the original equation, one needs also to specify a new boundary condition. To lowest order in the strains, one can rewrite Eq. (10) as

$$\nu_i = -\frac{\partial R_i}{\partial t} + d\,\frac{\partial \tau_{ij}}{\partial r_j}. \tag{11}$$

In order that the surface of the solid be unambiguously defined, we take as the boundary condition,

$$\nu_{s\perp} = -\left(\frac{\partial R_\perp}{\partial t}\right)_{\text{surface}} = \dot{l}, \tag{12}$$

where $\nu_{s\perp}$ is the perpendicular component of the surface velocity and l is the dimension of the solid body. By continuity, Eq. (5),

$$\nu_{s\perp} = \nu_\perp(\text{surface}), \tag{13}$$

the perpendicular component of the bulk velocity evaluated at the surface. Combining Eqs. (10)–(12) yields

$$d\left(\frac{\partial \tau_{\perp j}}{\partial r_j}\right)_{\text{surface}} = 0, \tag{14}$$

the dissipative term is required to vanish at the surface. One way to satisfy this condition is by letting $d \to 0$ at the surface, which states that the dislocations annihilate as they hit the surface. The formal solution to elasticity with a small plastic flow is obtained by putting Eq. (11) into Eqs. (5), (6), and (9) to obtain a closed theory for $\vec{R}$, ρ, and s.

Subject to the boundary condition (14) one can solve for the dissipative flow inherent in the Inglis solution by putting Eq. (4) into Eq. (11):

$$\nu_\alpha = -\frac{\mu d}{h^5}\,\frac{c^4 T}{8\mu}\,(\cosh 2\alpha\,\cos 2\beta - 1)\left(\frac{14}{3} - \frac{2}{3}\,p\right), \tag{15}$$

$$\nu_\beta = -\frac{\mu d}{h^5}\,\frac{c^4 T}{8\mu}\,(\sinh 2\alpha\,\sin 2\beta)\left(\frac{14}{3} - \frac{2}{3}\,p\right). \tag{16}$$

Here the tendency of the plastic flow is to distort the elliptical shape into a circular one (Fig. 2). The rate of blunting of the crack tip itself is

$$\nu_\alpha(\alpha = \alpha_0, \beta = 0) = \dot{a} = -\frac{\mu d}{4}\,\frac{T}{\mu}\,\frac{c^2}{b^3}\left(\frac{14}{3} - \frac{2}{3}\,p\right). \tag{17}$$

The time scale associated with rate of decrease of the tensile stress at the tip of a narrow crack ($a \gg b$) is given by

$$\frac{\sigma_{\beta\beta}}{\dot{\sigma}_{\beta\beta}} \approx \frac{a}{\dot{a}} \approx \frac{a^2 T^2}{d\mu_c^3}. \tag{18}$$

If one scales the cohesive strength with the bulk modulus, this simplifies to $a/\dot{a} \approx b^2/\mu d$. Clearly, depending on the value of d, plastic effects resist the sharpness of the crack tip; the value of the diffusion constant sets the time scale at which plastic effects dominate elastic ones and eliminate stress singularities. Elastic responses can be estimated to travel at the speed of sound in the material, with a characteristic time scale given by a/c_s, where c_s is the speed of sound in the solid. For most solids the time scale for elastic response of a micrometer-sized crack is about a nanosecond. If the elastic response is much more rapid than the dissipative one, the solid will behave as a brittle one. If dissipation dominates, the high elastic stress concentrations such as those characterizing a crack tip will never be realized. The ratio of these time scales determines a measure of the relative degree of brittleness of a material; namely, if

$$\frac{aT^2 c_s}{d\mu_c^3} > 1, \tag{19}$$

the material is brittle, and if the inequality is of opposite sense, the material is ductile. Note that as the cohesive strength of the solid increases the material becomes more ductile, and as d, the measure of inelastic deformation, increases, the material also becomes more ductile. Finally, for fixed material parameters, a larger geometric crack size will make the solid behave in a more brittle fashion. In fatigue experiments [9], the ductile time scale (18) should be compared to the frequency with which the externally applied stress is ramped up and down. If the periods are sufficiently long that elastic strains can be relaxed during the low-stress phase, brittle fracture will be suppressed.

A different approach to the issue of distinguishing brittleness and ductility, pioneered by Armstrong [10], compares the stress necessary to propagate a Griffith crack by cleavage to the stress required to nucleate dislocation loops at the crack tip. The comparison yields the dimensionless parameter $\gamma/\mu b_d$, where γ is the surface energy and b_d is the Burgers vector of the dislocation, which scales as the lattice spacing. The greater this Armstrong ratio, the more ductile the crystal, and vice versa. This comparison involves characterizing the microscopic nature of the cohesive forces and the dislocation structures, and the parameter rather successfully encapsulates the macroscopic effects of changes at the microstructural level. However, its extension to systems lacking crystalline symmetry is unclear, and the experimental determination of the microscopic parameters involved is nontrivial.

Independently, Kelly, Tyson, and Cottrell [11] defined the relative brittleness of a crystal by comparing the maximum

tensile stress and the maximum shear stress achieved in a given apparatus as the external load was increased. Depending on the load conditions and the crystalline structure, the crystal's cohesive strength or ideal shear strength would be reached first, resulting, respectively, in cleavage or plastic deformation. Rice and Thomson [12] explicitly modeled the production of a blunting dislocation at the crack tip (such that its slip plane contains the crack line). Their model specifies a mechanism by which the competition between crack propagation and plastic crack tip blunting can take place, and their rigorous calculation of this mechanism recovers the Armstrong criterion:

$$\frac{\gamma}{\mu b_d} > 7-10 \tag{20}$$

for ductile fracture. More recent approaches [13] generalize the Rice-Thomson calculation to consider geometrical aspects of dislocation emission and external loading via a Peierls-Nabarro framework. Introduction of the ''unstable stacking energy'' as a parameter determining the energy barrier to dislocation emission introduces the opportunity for atomistic refinements of the Rice-Thomson criterion above. The competition between brittle cleavage and dislocation emission has also been considered in dynamic fracture [14].

The expressions (20) and (19) above predict similar dependence of the brittleness of a solid on, e.g., the cohesive strength of the material, but Eq. (20) explicitly depends on the microscopic dislocation size. The constant d in Eqs. (18) and (19) above can presumably be written in terms of microscopic parameters for specific materials, but has been deduced from strictly thermodynamic, macroscopic reasoning. Thus the value of d can be determined from a simpler experiment, such as the creep of a bar under its own weight, where the stresses are low and the system is well described by elasticity, modified by a small dissipative correction. The rate of decrease of the height of a solid in a gravitational field [15], which is derived by using the solutions to Eq. (5)–(7) above and putting that solution into Eq. (11), is

$$\dot{l} \approx -d\,\frac{4}{3}\,\frac{\mu\rho g}{E}\,(1+\sigma), \tag{21}$$

where l is the height of the bar and E is Young's modulus. Measurement of the rate of creep of the bar thus yields d, which then sets the time scale in Eq. (18) for given crack dimensions. Rayleigh [16] observed that certain heat-treated specimens of marble, including some mantelpieces, would creep under their own weight on a time scale of weeks, while most marble samples showed no evidence of such deformation. Using Rayleigh's observations on the creep of such a marble mantelpiece [16] to find d from Eq. (21) and Griffith's estimate of the crack dimensions of intrinsic flaws in Eq. (18), one finds that the time scale for cracks to blunt is measured in picoseconds. That implies that specimens of such heat-treated marble should be considered candidates for failure by ductile deformation rather than by brittle fracture, which characterizes most marble. The observation of the sagging of lead pipes [17] over time leads to an estimate of the crack-blunting time scale of tens of picoseconds and to the classification of pure lead as a ductile material. In steel the diffusion constant is much lower; time-dependent deformation-mechanism maps for Type 316 stainless steel [17] suggest that the relevant time scale is microseconds, and therefore the transition from ductile to brittle behavior in fatigue experiments should occur at MHz frequencies. In these examples we have used values for d obtained at low stresses to estimate the response of a highly stressed region. In fact, if d is itself a function of the stress, the value which pertains to the crack tip differs from that measured in a creep experiment. However, the plastic deformation described by Eqs. (15) and (16) is a bulk flow phenomenon, involving regions of both high and low stress, and therefore the effective d, which is an average over an area much greater than the crack tip, should be reasonably well estimated by the creep-determined d.

The observation in many materials of a hardening transition from ductile to brittle behavior [3] as a solid is repetitively stressed suggests that the above formalism is conceptually incomplete. However, rather than applying the boundary condition above, which assumes that the concentration of dislocations vanishes at the surface of the crack, one can consider the scenario where dislocations cannot pass through the surface and annihilate. In this case we suppose that dislocations build up in a surface layer, so that d does not vanish at the surface. Then the boundary condition (14) implies that $\partial\tau_{\perp j}/\partial r_j = 0$ at the surface. In addition the existence of such a surface layer implies that there is a discontinuity in the perpendicular stress at the surface. If one solves the equations of elasticity for the equilibrium of an elliptical hole in a uniformly stressed plane, subject to the boundary conditions of vanishing shear stress and vanishing perpendicular gradient of the shear stress on the surface, the Inglis solution (1)–(4) is replaced by

$$\sigma_{\alpha\alpha} = \frac{T}{2}\,\frac{\sinh 2\alpha}{(\cosh 2\alpha - \cos 2\beta)^2}\left(2\cosh 2\alpha + -\frac{1}{3}\,(p-1)\right.$$
$$\left.\times\cosh 2\alpha_0 + \frac{1}{3}\,(p-7)\cos 2\beta\right), \tag{22}$$

$$\sigma_{\beta\beta} = \frac{T}{2}\,\frac{\sinh 2\alpha}{(\cosh 2\alpha - \cos 2\beta)^2}\left(2\cosh 2\alpha + \frac{1}{3}\,(p-1)\right.$$
$$\left.\times\cosh 2\alpha_0 + -\frac{1}{3}\,(p+5)\cos 2\beta\right), \tag{23}$$

$$\sigma_{\alpha\beta} = \frac{T}{6}\,(p-1)\,\frac{\sin 2\beta(\cosh 2\alpha - \cosh 2\alpha_0)}{(\cosh 2\alpha - \cos 2\beta)^2}, \tag{24}$$

which corresponds to displacements of

$$\delta R_\alpha = \frac{1}{h}\,\frac{c^2 T(p-1)}{8\mu}\left(\cosh 2\alpha - \frac{4}{3}\cos 2\beta + \frac{1}{3}\cosh 2\alpha_0\right) \tag{25}$$

and $\delta R_\beta = 0$. In the crack limit ($a \gg b$) both the perpendicular and tensile stresses at the crack tip become singular,

$$\sigma_{\alpha\alpha}(\alpha=\alpha_0, \beta=0) \approx \frac{(7-p)}{6}\,T\,\frac{a}{b}, \tag{26}$$

$$\sigma_{\beta\beta}(\alpha=\alpha_0,\beta=0)\approx\frac{(p+5)}{6}\,T\,\frac{a}{b}, \tag{27}$$

but since $p\approx 2$ for most materials, the tensile stress exceeds the perpendicular one.

The plastic flow associated with this solution which is obtained by using Eq. (25) in Eq. (11) vanishes identically. Thus when the boundary maintains a finite, steady distribution of dislocations, the resultant elastic field in the solid resists plastic deformation. This ''hardened'' state is then susceptible to fracture, since the stresses concentrated at the crack tip cannot be dissipated, and the dynamics are governed only by elastic forces. According to this model, the transition from ductility to brittleness as observed in work hardening need not, therefore, involve a bulk transformation of the material, but should be signaled by a detectably defect-riddled surface. In such cases, Eqs. (22)–(25), rather than the Inglis solution (1)–(4), should constitute the foundation of a theoretical investigation of fracture. A description of the hardening transition itself is much more complicated. That would require incorporating into the creep equation (11) a time-dependent diffusion constant d self-consistently determined as a function of the elastic stresses as dislocations accumulate in the solid.

Most modern approaches to fracture mechanics exploit the powerful mathematical techniques related to singular integral equations [18]. These approaches reduce the elliptical void to a line, and apply the boundary conditions of vanishing shear stress and perpendicular stress to a segment of length $2c$ (or equivalently $2a$) of the x axis. These equations imply a square-root stress singularity at the ends of the crack, $x=\pm a$, in both σ_{yy} and σ_{xx}. The singularity in the crack-opening stress, σ_{yy}, is often remedied by assuming the existence of a cohesive zone near the crack tip, where an attractive force between the faces of the crack balances the elastic stress and removes the singularity [19]. The underlying elastic model (i.e., without the cohesive zone) corresponds to a singular limit of the solutions (1)–(3) above, obtained by evaluating them at $\alpha_0=0$, $\beta=0$, and then taking $\alpha\to\alpha_0$. In this limit the perpendicular stress at $x=\pm a$ no longer vanishes; instead it is equal to the tensile stress, or, $\sigma_{xx}=\sigma_{yy}=Ta/b$, which diverges since the aspect ratio is infinite. The equivalence of the tensile and perpendicular stresses at the crack tip is an artifact of the awkward order of limits taken in Eqs. (1)–(3) to approach the infinitesimally wide crack, which occurs neither in the full Inglis solution [Eqs. (1)–(3)] nor in the work-hardened solution [Eqs. (22)–(24)]. However, this equivalence is preserved in the (static) cohesive zone model, which underlies many modern theories of dynamic fracture, whose goal is to investigate instabilities in crack propagation [20,21]. The artificial equivalence of the tensile and perpendicular stresses in this elastic model makes the direction of crack propagation ill defined. Clearly, the instabilities in the direction of crack propagation which result from this ambiguity must be regarded as distinct from true, dynamical deviations of the crack propagation from a straight line.

The dynamic instabilities associated with a moving Inglis crack remain to be investigated. In particular, the speed of crack propagation provides yet another time scale with which to compare the effects of plasticity on the elastic equations. For sufficiently rapid crack propagation plastic effects might distort the fractured trail of the solid, but never reach the crack tip itself. The steady-state profile of a ''crack tip'' in a ductile solid might give insight into the workings of failure by plastic deformation. One might ask whether the work-hardened surface possesses a stable crack profile in the dynamic state and from an engineering perspective consider effects of the environment, such as corrosion, on this profile [9]. Finally, given the dynamic equations describing a crack in a nearly elastic solid, one might consider the tantalizing possibility of macroscopically driven, oscillatory crack motion [22].

I am grateful to J. Langer, G. Mazenko, S. Putterman, and Z. Suo for comments and criticisms. This work is supported by the ITP's NSF Grant No. 94-07194.

[1] C. E. Inglis, Trans. Inst. Nav. Arch. **55**, 219 (1913).
[2] A. A. Griffith, Philos. Trans. R. Soc. London, Sec. A **221**, 163 (1921).
[3] R. W. K. Honeycombe, *The Plastic Deformation of Metals*, 2nd ed. (Arnold, London, 1984).
[4] E. N. da C. Andrade, Proc. R. Soc. London, Ser. A **84**, 1 (1910).
[5] L. D. Landau and E. M. Lifshitz, *Theory of Elasticity*, 3rd ed. (Pergamon, New York, 1986).
[6] C. Eckart, Phys. Rev. **73**, 373 (1948).
[7] P. D. Fleming and C. Cohen, Phys. Rev. B **13**, 500 (1976).
[8] R. Löfstedt, preceding paper, Phys. Rev. E **55**, 6719 (1997).
[9] S. Suresh, *Fatigue of Materials* (Cambridge, Cambridge, England, 1991).
[10] R. W. Armstrong, Mater. Sci. Eng. **1**, 251 (1966).
[11] A. Kelly, W. R. Tyson, and A. H. Cottrell, Philos. Mag. **15**, 567 (1967).
[12] J. R. Rice and R. Thomson, Philos. Mag. **29**, 73 (1974).
[13] J. R. Rice, G. E. Beltz, and Y. Sun, in *Topics in Fracture and Fatigue*, edited by A. S. Argon (Springer, New York, 1992), p. 1.
[14] L. B. Freund and J. W. Hutchinson, J. Mech. Phys. Solids **33**, 169 (1985); A. S. Argon, Acta Metall. **35**, 185 (1987).
[15] S. P. Timoshenko and J. N. Goodier, *Theory of Elasticity* (McGraw-Hill, New York, 1970).
[16] Lord Rayleigh, Proc. R. Soc. London, Ser. A **144**, 266 (1934).
[17] H. J. Frost and M. F. Ashby, *Deformation-Mechanism Maps* (Pergamon, New York, 1982).
[18] L. B. Freund, *Dynamic Fracture Mechanics* (Cambridge, Cambridge, England, 1990).
[19] G. I. Barenblatt, Adv. Appl. Math. **7**, 55 (1962).
[20] E. H. Yoffe, Philos. Mag. **42**, 739 (1951).
[21] E. S. C. Ching, J. S. Langer, and H. Nakanishi, Phys. Rev. Lett. **76**, 1087 (1996).
[22] J. W. Obreimoff, Proc. R. Soc. London, Ser. A **127**, 290 (1930).